CMNE/CILAMCE 2007
Porto, 13-15 Junho, 2007

CRACK CONSTITUTIVE MODEL TO SIMULATE THE BEHAVIOR OF FIBER REINFORCED CONCRETE STRUCTURES FAILING IN PUNCHING

A. Ventura Gouveia [1]*, Joaquim Barros[2], Álvaro Azevedo[3] and J. Sena Cruz [2]

1: Civil Engineering Department
School of Technology
Polytechnic Institute of Viseu
Campus de Repeses, 3504-510 Viseu, PORTUGAL
e-mail: ventura@dcivil.estv.ipv.pt, web: http://www.dcivil.estv.ipv.pt/dep/dcivil

2: Civil Engineering Department
School of Engineering
University of Minho
Campus de Azurém, 4800-058 Guimarães, PORTUGAL
e-mail: barros@civil.uminho.pt, jsena@civil.uminho.pt
web: http://www.civil.uminho.pt/composites

3: Civil Engineering Department
Faculty of Engineering
University of Porto
Rua Dr. Roberto Frias, s/n 4200-465 Porto, PORTUGAL
e-mail: alvaro@fe.up.pt, web: http://www.fe.up.pt/~alvaro

Keywords: Crack Constitutive Model, Punching, Steel Fiber Reinforced Self-Compacting Concrete, Material Nonlinear Analysis, Finite Element Method, Inverse Analysis.

Summary. *For some structural applications, mainly with redundant supports, adding fibers to concrete can be an economic strategy, especially when shear brittle failure mode has a high risk of occurrence. In the present work, a crack constitutive model is proposed to simulate localized failure modes due to punching. The performance of the developed constitutive model was appraised by simulating the behavior observed in punching tests with lightweight panel prototypes of steel fiber reinforced self-compacting concrete (SFRSCC). The values of the parameters required by fracture mode I of the SFRSCC were obtained by inverse analysis.*

1. INTRODUCTION

Recent developments in the fiber reinforced concrete technology showed that the addition of a small content of hooked end steel fibers to a self-compacting concrete resulted in a high strength and ductile material with a significantly increased flexural and punching resistance [1]. The mechanical performance of the developed steel fiber reinforced self-compacting concrete (SFRSCC) is mainly due to the proposed innovative mix design strategy. In the determination of the proportions of each aggregate in the final solid skeleton the presence of the steel fibers and their specificities (fiber content and fiber aspect-ratio) were taken into account [1]. The developed SFRSCC was used to manufacture lightweight pre-cast panels for building façades, with the geometry schematically represented in Figure 1. Since the SFRSCC layer at the lighter parts of the panel is only 30 mm thick, its resistance to punching was assessed from experimental tests [2].

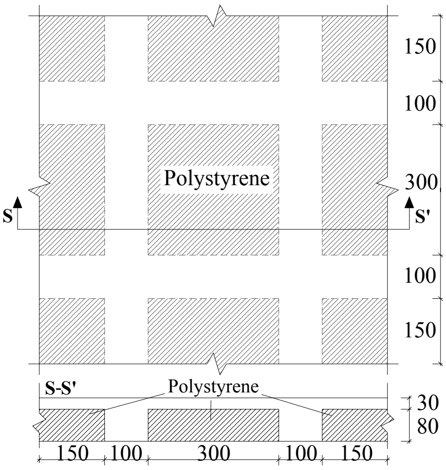

Figure 1. Lightweight SFRSCC panel (dimensions in mm).

Modeling the material nonlinear behavior of a laminar structure failing in punching is still a challenge in the computational mechanics domain. A 3D crack constitutive model can be implemented, using solid finite elements [3], but the numerical stability is compromised when softening crack constitutive diagrams are adopted for modeling all three fracture modes that are activated during the propagation of a crack. Furthermore, according to the knowledge of the authors of the present work, a well accepted strategy for evaluating the softening laws that simulate fracture modes II and III is not yet available.

In the present paper a simple but accurate model is proposed to simulate the behavior of cement based laminar structures failing in bending and in shear. Special emphasis is put on the analysis of structures failing in punching. The developed model is based on finite element techniques and was implemented in the FEMIX computer code [4]. The Reissner-Mindlin theory was used in the context of layered shells. By considering the nonlinear behavior of each layer, crack propagation along the thickness of these structures can be simulated [5]. Fracture mode I was modeled by a crack stress *vs.* crack strain tri-linear diagram, whose

defining parameters were obtained from inverse analysis [6], considering the force-deflection curves registered in three-point notched SFRSCC beam tests carried out according to the RILEM TC 162-TDF recommendations [7].
The model is described and its performance is appraised using the results obtained from punching tests carried out with representative parts of the developed SFRSCC panel.

2. NUMERICAL MODEL

2.1. Introduction

Previous works showed that the Reissner-Mindlin theory for shell structures [5] is capable of predicting with high accuracy the behavior of laminar concrete structures up to failure [8]. However, when these structures fail in shear, this type of approach seems to be inadequate, since the model predicts cracks that are orthogonal to the middle surface of the shell, which is not the real orientation of the cracks formed in the experimental tests. To explore the possibility of using the Reissner-Mindlin shell theory to simulate the material nonlinear behavior of concrete laminar structures failing in punching, a softening law was introduced for modeling the two out-of-plane shear stress-strain diagrams. To simulate concrete cracking a multi-fixed smeared crack model was implemented [9]. Fracture mode I is modeled by a crack stress *vs.* crack strain diagram, whose defining parameters were determined from inverse analysis based on the results obtained in flexural tests. The specimens used in these tests and the panels studied with the present model were of the same age (seven days).

2.2. Formulation

When the behavior of a material is considered to be linear elastic the constitutive matrix ($\underline{D}$) does not depend on the stress or strain level. However, when the material behaves nonlinearly, this matrix can not be assumed as constant. Numerically, it may be considered that $\underline{D}$ assumes constant values for very small stress and strain increments and, consequently, the constitutive law may be defined as follows,

$$\Delta\underline{\sigma} = \underline{D} \ \Delta\underline{\varepsilon} \tag{1}$$

where $\Delta\underline{\sigma}$ represents the stress increment, $\Delta\underline{\varepsilon}$ is the strain increment and $\underline{D}$ is the tangent constitutive matrix.
In the context of the Reissner-Mindlin shell theory, the stress vector has five components,

$$\underline{\sigma} = \left\{\sigma_1, \sigma_2, \tau_{12}, \tau_{23}, \tau_{31}\right\}^T \tag{2}$$

where the first three constitute the in-plane components ($\underline{\sigma}_{mf}$) and the last two are the out-of-plane or transverse shear components ($\underline{\sigma}_s$). In a similar way, the strain vector also has five independent components,

$$\underline{\varepsilon} = \{\varepsilon_1, \varepsilon_2, \gamma_{12}, \gamma_{23}, \gamma_{31}\}^T \tag{3}$$

Since the thickness of the tested structural elements is small, concrete is assumed to behave in linear elastic regime in compression. In tension the behavior of the concrete is considered linear until the tensile strength is reached. The constitutive matrix is composed of two parts, the first one being associated with the in-plane (membrane and flexural) deformation components ($\underline{D}^{co}_{mf,e}$), and the second one associated with the out-of-plane (transverse shear) deformation ($\underline{D}^{co}_{s,e}$), both including concrete (*co*) properties in elastic regime (*e*). Therefore, the concrete elastic constitutive matrix may be described as

$$\underline{D}^{co} = \begin{bmatrix} \underline{D}^{co}_{mf,e} & \underline{0} \\ \underline{0} & \underline{D}^{co}_{s,e} \end{bmatrix} \tag{4}$$

where $\underline{D}^{co}_{mf,e}$ and $\underline{D}^{co}_{s,e}$ may be defined as

$$\underline{D}^{co}_{mf,e} = \frac{E_c}{1-\nu^2} \begin{bmatrix} 1 & \nu & 0 \\ \nu & 1 & 0 \\ 0 & 0 & \frac{1-\nu}{2} \end{bmatrix} \tag{5}$$

$$\underline{D}^{co}_{s,e} = F\, G_c \begin{bmatrix} 1 & 0 \\ 0 & 1 \end{bmatrix} \tag{6}$$

where E_c is the Young's modulus, G_c the transverse elasticity modulus and ν is the Poisson's ratio, considering the concrete in elastic regime. The factor F is a shear corrective constant, associated with the assumption of constant out-of-plane shear stresses, when, in isotropic materials, they assume a parabolic distribution. For rectangular sections, $F = 5/6$.

When the tensile strength of concrete is reached, the material starts to behave nonlinearly, and the constitutive matrix is changed.

In the present work, to simulate the loss of strength associated with the strain-softening behavior of concrete in tension and in out-of-plane shear, the in-plane deformation components ($\underline{D}^{co}_{mf,e}$) and the out-of-plane shear deformation components ($\underline{D}^{co}_{s,e}$) of the constitutive matrix are modified. The strain-softening behavior of concrete in tension is simulated by a stress-strain tri-linear diagram, as represented in Figure 2, relating the crack stress and crack strain orthogonal to the crack plane. The out-of-plane shear strain-softening behavior of concrete is simulated by the diagram represented in Figure 3, relating a generic out-of-plane shear stress with the corresponding out-of-plane shear strain.

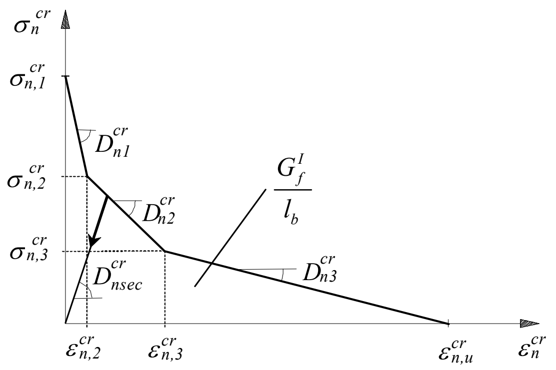

Figure 2. Tri-linear stress-strain diagram.

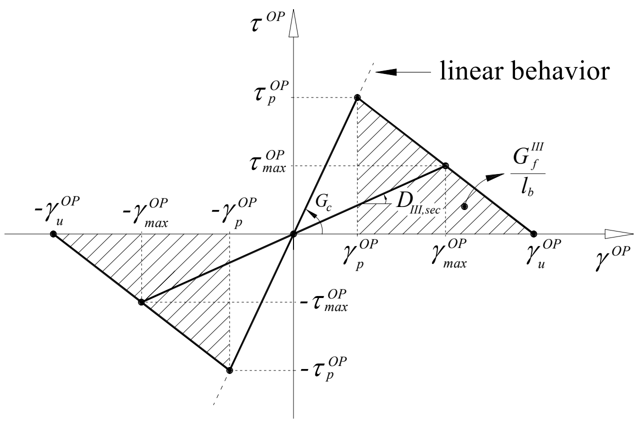

Figure 3. Generic out-of-plane (OP) shear stress-strain diagram.

When the tensile strength is reached at an integration point (IP) of a finite element, the portion of concrete included in its influence area changes from the uncracked to the cracked state. Using the multi-fixed smeared crack concept [10], the component $\underline{D}_{mf,e}^{co}$ of the concrete constitutive matrix $\underline{D}^{co}$ is replaced by $\underline{D}_{mf}^{crco}$, determined with the following equation [9],

$$\underline{D}_{mf}^{crco} = \underline{D}_{mf,e}^{co} - \underline{D}_{mf,e}^{co}\left[\underline{T}^{cr}\right]^T \left(\underline{D}^{cr} + \underline{T}^{cr}\,\underline{D}_{mf,e}^{co}\left[\underline{T}^{cr}\right]^T\right)^{-1} \underline{T}^{cr}\,\underline{D}_{mf,e}^{co} \tag{7}$$

where $\underline{T}^{cr}$ represents the transformation matrix from the crack local coordinate system to the element local coordinate system, and $\underline{D}^{cr}$ represents the crack constitutive matrix, as described in the following equations

$$\underline{T}^{cr} = \begin{bmatrix} \cos^2\theta & \sin^2\theta & 2\sin\theta\cos\theta \\ -\sin\theta\cos\theta & \sin\theta\cos\theta & \cos^2\theta - \sin^2\theta \end{bmatrix} \tag{8}$$

$$\underline{D}^{cr} = \begin{bmatrix} D_I^{cr} & 0 \\ 0 & D_{II}^{cr} \end{bmatrix} \tag{9}$$

In Eq. (8), θ is the angle between the crack local coordinate system and the finite element coordinate system (see Figure 4). In Eq. (9), D_I^{cr} and D_{II}^{cr} represent, respectively, the constitutive components corresponding to the crack opening mode I (normal) and crack sliding mode II (in-plane shear). The fracture mode I modulus, D_I^{cr}, is defined in Figure 2, where α_i and ξ_i are the parameters that define the shape of the crack normal stress *vs.* crack normal strain diagram. The ultimate crack strain ($\varepsilon_{n,u}^{cr}$) is defined as a function of α_i and ξ_i parameters, of fracture energy (G_f^I), tensile strength (f_{ct}) and crack band width (l_b), as follows [5],

$$\varepsilon_{n,u}^{cr} = \frac{2}{\xi_1 + \alpha_1 \xi_2 - \alpha_2 \xi_1 + \alpha_2} \cdot \frac{G_f^I}{f_{ct} l_b} \tag{10}$$

where $\alpha_1 = \sigma_{n,2}^{cr} / \sigma_{n,1}^{cr}$, $\alpha_2 = \sigma_{n,3}^{cr} / \sigma_{n,1}^{cr}$, $\xi_1 = \varepsilon_{n,2}^{cr} / \varepsilon_{n,ult}^{cr}$ and $\xi_2 = \varepsilon_{n,3}^{cr} / \varepsilon_{n,ult}^{cr}$.

The fracture mode II modulus, D_{II}^{cr}, is obtained from,

$$D_{II}^{cr} = \frac{\beta}{1-\beta} G_c \tag{11}$$

$$\beta = \left(1 - \frac{\varepsilon_n^{cr}}{\varepsilon_{n,ult}^{cr}}\right)^{p_1} \tag{12}$$

where β is the shear retention factor, defined as a function of the actual crack normal strain (ε_n^{cr}) and the ultimate crack normal strain ($\varepsilon_{n,ult}^{cr}$). When a linear decrease of β with the increase of ε_n^{cr} is assumed, then $p_1 = 1$. Larger values of the exponent p_1 correspond to a faster decrease of the parameter β [5]. The use of a softening constitutive law to model the in-plane crack shear stress transfer can improve the accuracy of the simulation of structures failing in shear [11]. However, the simultaneous presence of softening laws to model fracture modes I and II introduces additional difficulties on assuring convergence during the loading procedure of a material nonlinear analysis.

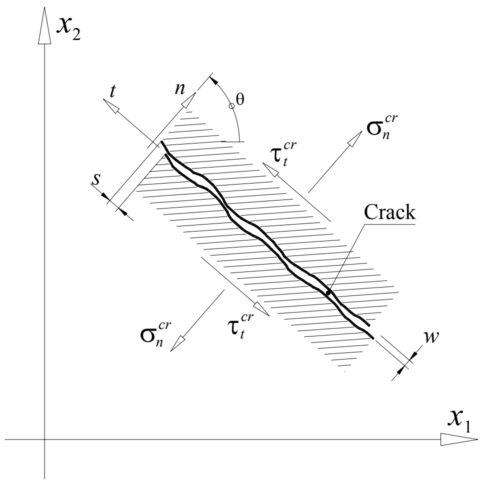

Figure 4. Crack stress components, relative displacements and local coordinate system of the crack.

The out-of-plane shear behavior is assumed to be linear elastic until the tensile strength is reached. When the portions of concrete associated with the IP change from uncracked to

cracked state the out-of-plane shear stresses are stored and the relation between each out-of-plane shear stress-strain ($\tau_{23} - \gamma_{23}$ and $\tau_{31} - \gamma_{31}$) follow an independently softening behavior as shown in Figure 3.
The component $\underline{D}_{s,e}^{co}$ of the concrete constitutive matrix $\underline{D}^{co}$ of Eq. (4) is replaced with $\underline{D}_{s}^{crco}$, which is defined by

$$\underline{D}_{s}^{crco} = \begin{bmatrix} D_{III,\sec}^{23} & 0 \\ 0 & D_{III,\sec}^{31} \end{bmatrix} \tag{13}$$

where

$$D_{III,\sec}^{23} = \frac{\tau_{23,\max}}{\gamma_{23,\max}}\ ;\ D_{III,\sec}^{31} = \frac{\tau_{31,\max}}{\gamma_{31,\max}} \tag{14}$$

according to a secant approach (see Figure 3).
For each out-of-plane shear component, the peak shear strain is calculated using the stored peak shear stress at crack initiation and the concrete elastic shear modulus

$$\gamma_{23,p} = \frac{\tau_{23,p}}{G_c}\ ;\ \gamma_{31,p} = \frac{\tau_{31,p}}{G_c} \tag{15}$$

Each out-of-plane ultimate shear strain is defined as a function of the out-of-plane peak shear strain (γ_p^{OP}), the out-of-plane shear strength (τ_p^{OP}), the mode III (out-of-plane) fracture energy (G_f^{III}) and the crack band width (l_b), as follows

$$\gamma_{23,u} = \gamma_{23,P} + \frac{2G_f^{III}}{\tau_{23,p}\ l_b}\ ;\ \gamma_{31,u} = \gamma_{31,P} + \frac{2G_f^{III}}{\tau_{31,p}\ l_b} \tag{16}$$

In the present approach it is assumed that the crack band width used for assuring mesh independence when modeling fracture mode I can also be used to define the dissipated energy in the out-of-plane fracture process.

3. ASSESSING THE FRACTURE MODE I CRACK CONSTITUTIVE LAW FROM INVERSE ANALYSIS

To obtain the values of α_i, ξ_i, G_f, f_{ct} that define the tri-linear stress-strain softening diagram (see Figure 2), an inverse analysis was performed using the force-deflection relationships recorded in the three-point notched SFRSCC beam tests, carried out according to RILEM TC 162-TDF recommendations at the age of seven days [6]. The inverse analysis consists on the evaluation of the values of these parameters, leading to the minimization of the ratio between the area limited by the experimental and the numerical curves and the area underneath the experimental curve. The numerical curve corresponds to the results obtained

by means of a FEM analysis (see Figure 5a), where the specimen, the loading and the support conditions were simulated in agreement with the experimental flexural test setup. In this context, the specimen was discretized using a mesh of 8 noded 'serendipity' plane stress finite elements. The Gauss-Legendre integration scheme with 2×2 points was used in all elements, with the exception of those located at the specimen symmetry axis, where 1×2 points were used. Linear elastic material behavior was assumed in all the elements, with the exception of those located above the notch and along the specimen symmetry axis, where elastic-cracked behavior in tension was considered. The crack band width, l_b, was assumed to be 5 mm, which corresponds to the width of the elements above the notch.
In Figure 5b the results experimentally obtained in the flexural tests are compared with those resulting from the numerical model for the same test setup. Although not exactly coincident, there exists a good agreement between the experimental and the numerical curves. The values assumed for the fracture parameters, α_i, ξ_i, and G_f, that resulted in the obtained numerical curve represented in Figure 5b, are listed in Table 1.

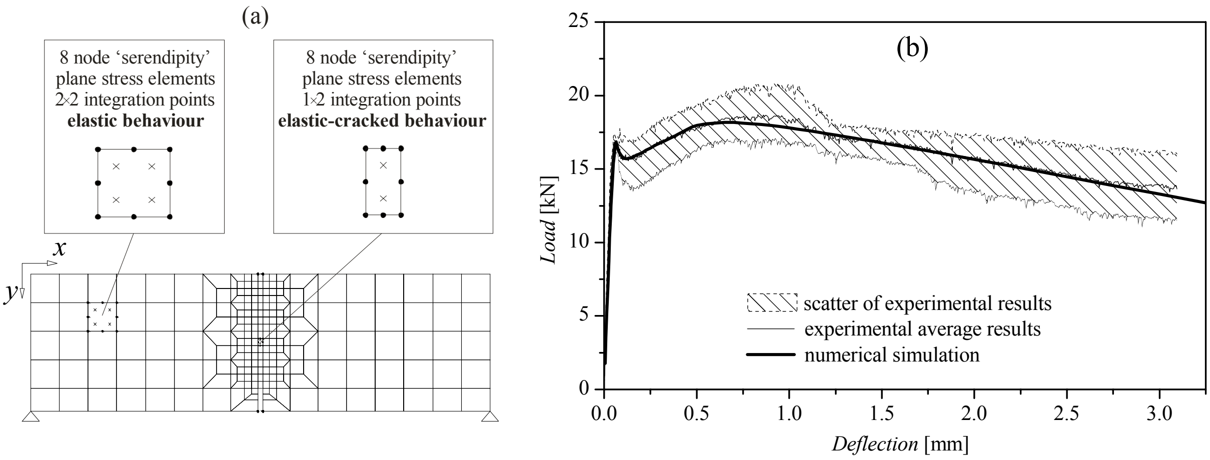

Figure 5. Three-point notched beam flexural test at 7 days: (a) FEM mesh used in the numerical simulation and (b) obtained results.

4. MODEL APPRAISAL

The performance of the proposed constitutive model is assessed by simulating the behavior observed in a punching test with lightweight panel prototype of SFRSCC. The test layout and the test setup are represented in Figure 6. The finite element idealization, load and support conditions used in the numerical simulation of the punching test are shown in Figure 7. Only one quarter of the panel was used in the simulation due to double symmetry. Serendipity 8 noded Mindlin shell layered elements with 2×2 Gauss-Legendre integration scheme were used. The panel thickness of 110 mm was decomposed in 11 layers of equal thickness. In the lightweight zone (shaded elements in Figure 7) the first 9 layers correspond to the polystyrene material and only the last 3 layers correspond to SFRSCC. The dashed line represents the support of the panel, which was simulated with line springs with "infinite" stiffness in compression and null strength in tension, in order to simulate the loss of contact between the panel and the support during the loading process.

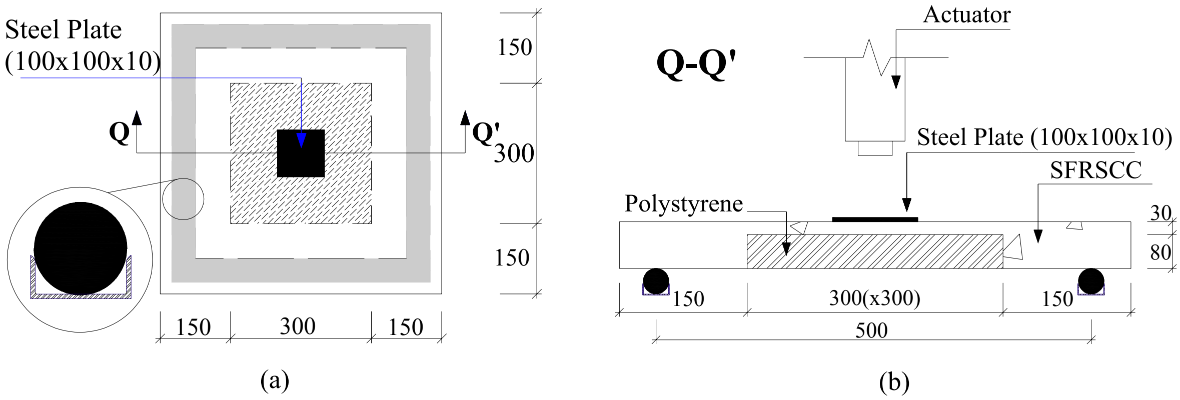

Figure 6. (a) Test panel prototype for the punching resistance and (b) test setup (dimensions in mm).

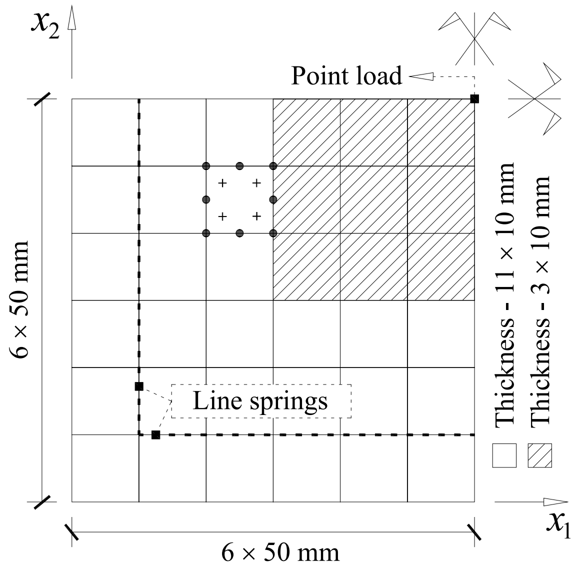

Figure 7. Geometry, mesh, load and support conditions used in the numerical simulation of the punching test.

The concrete properties used in the simulation of the punching test are listed in Table 1. To evaluate the performance of the proposed model two numerical simulations were carried out. The former considers a linear behavior for both out-of-plane shear components. The latter considers a softening behavior in both out-of-plane shear components when the SFRSCC cracks.

Poisson's ratio	$\nu = 0.15$
Initial Young's modulus	$E_c = 31000.0\ \mathrm{N/mm^2}$
Compressive strength	$f_c = 52.0\ \mathrm{N/mm^2}$
Tri-linear tension softening diagram of plain concrete	$f_{ct} = 3.5\ \mathrm{N/mm^2}$; $G_f^I = 0.08732\ \mathrm{N/mm}$; $\xi_1 = 0.072$; $\alpha_1 = 0.15$; $\xi_2 = 0.4432$; $\alpha_2 = 0.09$
Tri-linear tension softening diagram of SFRSCC	$f_{ct} = 3.5\ \mathrm{N/mm^2}$; $G_f^I = 4.3\ \mathrm{N/mm}$; $\xi_1 = 0.009$; $\alpha_1 = 0.5$; $\xi_2 = 0.15$; $\alpha_2 = 0.59$
Fracture energy (Mode III) used in the out-of-plane shear stress-strain diagram	$G_f^{III} = 3.0\ \mathrm{N/mm}$
Parameter defining the mode I fracture energy available to the new crack	$p_2 = 2$
Shear retention factor	*Exponential* ($p_1 = 2$)
Crack band width	*Square root of the area of the integration point*
Threshold angle	$\alpha_{th} = 30^{\circ}$

Table 1. Concrete properties used in the simulation of the punching test.

In Figure 8 the numerically obtained relations between the force and the deflection in the center of the test panel is compared with the one recorded in the experimental test. In this figure it can be observed that both numerical simulations have practically the same pre-peak response. However, the post-peak response differs significantly. When linear behavior is assumed for both out-of-plane shear components, the force increases up to 60 kN and only for a deflection of 9.6 mm a structural softening occurs, but with a very smooth load decay. The behavior predicted by this numerical simulation after a deflection of about 3 mm differs significantly from the experimental response. When a softening behavior in both out-of-plane shear components is adopted the numerical model predicts with high accuracy the behavior that was experimentally observed. The value of the mode III fracture energy used to define the out-of-plane shear stress-strain softening diagram has no experimental support. This value was estimated in order to assure the abrupt load decay observed experimentally at a deflection of about 3 mm. A value of $G_f^{III} = 3.0\ \mathrm{N/mm}$ was adopted. An increase of G_f^{III} causes the occurrence of the abrupt load decay at a larger deflection.

To estimate the contribution of fiber reinforcement to the punching resistance, a numerical simulation was performed adopting for the fracture mode I the parameters indicated in Table 1, which correspond to plain concrete of compressive strength matching the developed SFRSCC. Comparing the curves in Figure 8 it can be concluded that fibers not only increased significantly the punching resistance, but also, and especially, improved the ductility.

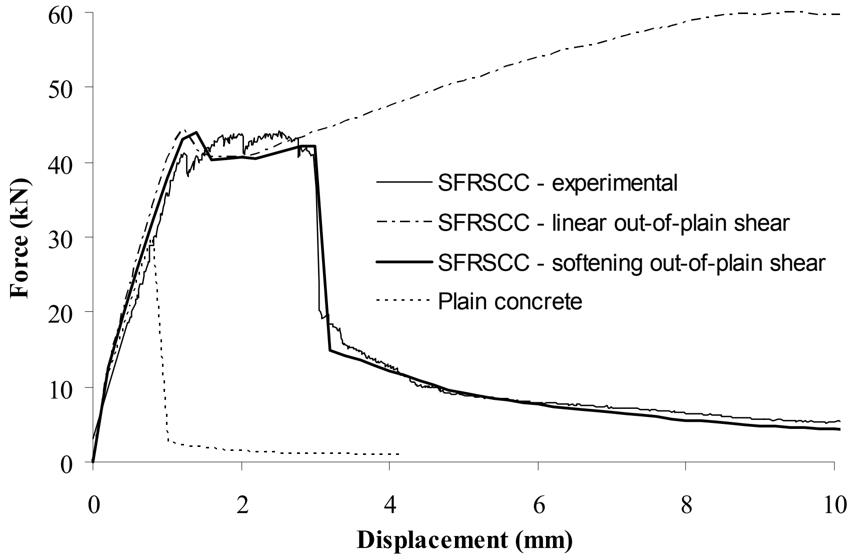

Figure 8. Relationship between the force and the deflection at the center of the test panel.

Figure 9 represents the vertical displacement field for a deflection of 10 mm in the center of the panel for the case of the numerical simulation considering out-of-plane shear softening. The accentuated gradient of vertical displacements matches with high precision the experimentally observed location of the interception of the punching failure surface with the top panel face (see Figure 10). This evidences the capability of the developed approach in the simulation of this complex failure mode.

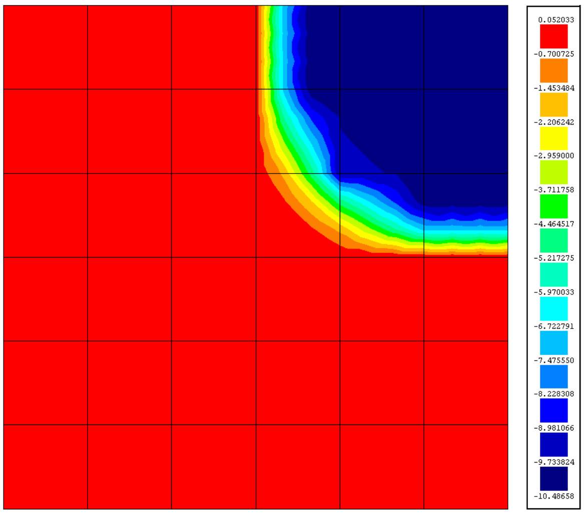

Figure 9. Vertical displacement field (in mm) for the numerical simulation with out-of-plane shear softening (for a deflection of 10 mm in the center of the panel).

Figure 10. Punching critical contour.

5. CONCLUSIONS

In the present work a simple but accurate model whose purpose is the simulation of the behavior of cement based laminar structures failing in bending and in shear is proposed. The developed model is based on the finite element method and was implemented in the FEMIX computer code. The Reissner-Mindlin theory was used in the context of layered shells. The crack propagation along the thickness of these structures can be simulated by considering the nonlinear behavior of each layer. The parameters of the fracture mode I were determined from inverse analysis using the force-deflection relationship obtained in three-point notched beam tests, carried out according to RILEM TC 162-TDF recommendations. This is a very important point since this type of test is much simpler and faster to execute than the direct tensile test. To simulate the out-of-plane strain gradient that occurs in punching tests, a softening diagram was proposed to model, after crack initiation, both out-of-plane shear stress-strain constitutive laws.
The performance of the model is appraised by using the results obtained in the punching test with lightweight panel prototypes of steel fiber reinforced self-compacting concrete (SFRSCC). A very good agreement between the experimental results and the proposed model is observed. It can be concluded that the present model is capable of simulating the behavior of cement based laminar structures failing in bending and in shear.

ACKNOWLEDGMENTS

The authors wish to acknowledge the support provided by the Portuguese Science and Technology Foundation (FCT) by means of the project POCTI/ECM/57518/2004 “FICOFIRE - High performance fiber reinforced concrete of enhanced fire resistance”. The first author acknowledges the financial support of FCT, PhD Grant number SFRH/BD/23326/2005.

REFERENCES

[1] Barros, J.A.O.; Pereira, E.B.; Santos, S.P.F., “Lightweight panels of steel fiber reinforced self-compacting concrete”, *Journal of Materials in Civil Engineering, 19(4)*, 2007.

[2] Barros, J.A.O.; Pereira, E.B.; Cunha, V.M.C.F.; Ribeiro, A.F.; Santos, S.P.F.; Queirós, P.A.A.A.V. “PABERFIA- Lightweight sandwhich panels in steel fiber reinforced self compacting concrete." *Technical Report 05-DEC/E-29*, Dep. Civil Eng., School of Eng. University of Minho, 63 pp., 2005

[3] Barzegar, Fariborz and Maddipudi, Srinivas, “Three-dimensional modeling of concrete structures. I: Plain Concrete”, *Journal of Structural Engineering, 123(10)*, pp. 1339-1346, October 1997.

[4] Azevedo A.F.M.; Barros J.A.O.; Sena-Cruz J.M.; Ventura-Gouveia A., "Software no ensino e no projecto de estruturas" (Educational software for the design of structures). In: *Proceedings of the III Engineering Luso-Mozambican Congress*, Maputo, Mozambique, pp. 81-92, 2003. (in Portuguese). <http://civil.fe.up.pt/pub/people/alvaro/pdf/2003_Mocamb_Soft_Ens_Proj_Estrut.pdf>

[5] Barros, J.A.O., "Behavior of fiber reinforced concrete - experimental and numerical analysis", *PhD Thesis*, Civil Eng. Dept., FEUP, Portugal, 1995. (in Portuguese).

[6] Pereira, E.B.; Barros, J.A.O.; Cunha, V.M.C.F.; Santos S.P.F., "Compression and bending behavior of steel fiber reinforced self-compacting concrete", *Third International Conference Construction Materials: Performance, Innovations and Structural Implications*, Vancouver, CD, 22-24 August 2005.

[7] RILEM TC 162-TDF. "Test and design methods for steel fibre reinforced concrete - Final Recommendation." *Materials and Structures 35(253)*, pp. 579-582, 2002.

[8] Barros, J.A.O. and Figueiras, J.A., "Nonlinear analysis of steel fibre reinforced concrete slabs on grade", *Computers & Structures Journal*, *79(1)*, pp. 97-106, January 2001.

[9] Sena-Cruz, J.M., "Strengthening of concrete structures with near-surface mounted CFRP laminate strips.", *PhD Thesis*, Department of Civil Engineering, University of Minho, 2004, <http://www.civil.uminho.pt/composites>

[10] Rots, J.G., "Computational modeling of concrete fracture", Dissertation, Delft University of Technology, 1988.

[11] Rots, J.G. and de Borst, R., "Analysis of mixed-mode fracture in concrete", *Journal of Engineering Mechanics*, ASCE, *113(11)*, pp. 1739-1758, 1987.